Multiphonon Relaxation of Rare-Earth Ions in Yttrium Orthoaluminate*

M. J. Weber
Raytheon Research Division, Waltham, Massachusetts 02154
(Received 1 February 1973)

Nonradiative relaxation by multiple-phonon emission was investigated for excited electronic states of rare-earth ions in $YAlO_3$. Ions studied included Nd^{3+}, Eu^{3+}, Ho^{3+}, Er^{3+}, and Tm^{3+}. Rates of multiphonon emission were determined from the difference of measured excited-state lifetimes and calculated radiative lifetimes. Electric dipole transition probabilities were computed using Judd–Ofelt intensity parameters for rare earths in $YAlO_3$. Multiphonon decay rates, measured for seventeen different levels with energies to the next-lower level ranging from 1400 to 4700 cm^{-1}, exhibited an approximately exponential dependence on energy gap ΔE given by $W(0)e^{-\alpha\Delta E}$, where $W(0)=5\times10^{9}\,sec^{-1}$ and $\alpha=4.6\times10^{-3}$ cm. Exceptions to the exponential law occur only when selection rules severely restrict the number of terms in the ion-lattice interaction active in inducing transitions. The phonon frequency distribution and ion-phonon coupling in $YAlO_3$ were examined from infrared, Raman, and vibronic spectra. Although phonon energies range up to 750 cm^{-1}, measurements of the temperature dependence of multiphonon emission indicate that phonons of energies $\sim$550–600 cm^{-1} make the dominant contribution to the relaxation at temperatures 77–700 °K.

I. INTRODUCTION

Nonradiative relaxation between electronic states of rare earths in crystals occurs by the emission or absorption of phonons. Whereas relaxation between crystalline Stark levels of a J manifold by one- or two-phonon processes is very fast and quickly establishes a Boltzmann population distribution, relaxation between J manifolds usually requires the participation of several phonons to conserve energy and hence proceeds at slower rates. The theory of high-order multiphonon processes for relaxation of $4f^n$ states of rare earths has been developed by several authors.[1–4] Experimentally, the rates of multiphonon emission from J manifolds have been measured for rare earths in several different host lattices.[2,5–12] The results of these studies demonstrate that for a given crystal, the most critical factor affecting the rate of multiphonon emission is the energy gap to the next-lower level. The detailed properties of the individual electronic states and the phonon modes involved are, with rare exceptions, averaged out. Measurements of the temperature dependence of the decay rates reveal further that relaxation occurs predominantly via high-energy optical phonons. Finally, since the energy separations of J states exhibit only small changes with host, differences in the rate of nonradiative decay from a given rare-earth level arise from the phonon frequency distribution of the host lattice and the strength of the ion-lattice coupling.

In this paper nonradiative decay by multiphonon emission is investigated for J states of trivalent rare earths in yttrium orthoaluminate. The approach used to determine the multiphonon emission rates is one applied previously[7–10] wherein calculated radiative decay rates are subtracted from measured total decay rates. In a preceding paper,[13] hereafter referred to as I, the optical spectra of rare earths in $YAlO_3$ were measured and phenomenological intensity parameters derived. These parameters are used to compute the spontaneous emission probabilities from excited states of interest.

From studies of seventeen excited states of five different ions, multiphonon decay rates in $YAlO_3$ are found to exhibit an approximate exponential dependence on energy gap to the next-lower level. Selection rules are reviewed and account for exceptions to the exponential law. The highest-energy phonons, which can conserve energy in the lowest-order process, are generally considered to make the dominant contribution to multiphonon relaxation.[2] In $YAlO_3$, the relaxation appears to arise principally from more numerous and/or more strongly coupled lower-energy phonons. This was established from comparisons of measured temperature dependences for multiphonon emission and temperature dependences predicted using a simplified single-frequency phonon model. Information about the extent of the phonon frequency distribution and the relative strength of the ion-phonon coupling was obtained from infrared, Raman, and vibronic spectra of $YAlO_3$.

II. EXPERIMENTAL APPROACH

A rare-earth ion in an excited state i decays with a lifetime τ given by

$$\frac{1}{\tau_i}=\sum_j (A_{ij}+W_{ij}) \quad , \tag{1}$$

where A and W are the probabilities for radiative and nonradiative decay, respectively, and the sum-

mation is over all terminal states j. Radiative processes include purely electronic and phonon-assisted vibronic transitions. Nonradiative processes include transitions by phonon emission or absorption and by energy migration and/or transfer arising from ion-ion interactions. Several approaches involving different combinations of measurements of lifetimes, absorption and fluorescence intensities, and quantum efficiencies have been used to determine nonradiative transition probabilities.[2,7,14–16] Here the radiative decay probabilities A_{ij} are calculated and subtracted from the measured total decay probability $1/\tau_i$ to find W.

The theory and treatment of radiative transitions for rare earths in crystals are reviewed in I.[13] Transitions are of electric and magnetic dipole character. The probability for spontaneous emission of dipole radiation between two J levels is given by

$$A(aJ;bJ') = [64\pi^4\nu^3\chi/3hc(2J+1)]\,S(aJ;bJ') \quad , \tag{2}$$

where ν is the frequency and χ is a correction factor for the refractive index of the host medium. For electric dipole transitions, χ is approximated by $n(n^2+2)^2/9$; for magnetic dipole transitions, $\chi = n^3$. In the Judd-Ofelt theory,[17,18] the line strengths for electric-dipole transitions between SLJ states is expressed as a sum of products of matrix elements of tensor operators $\underline{U}^{(\lambda)}$ and phenomenological intensity parameters Ω_λ of the form

$$S_{ed}(aJ;bJ') = e^2 \sum_{\lambda=2,4,6} \Omega_\lambda (f^N \alpha SLJ||\underline{U}^{(\lambda)}||f^N \alpha' S'L'J')^2 \quad . \tag{3}$$

The line strength for magnetic-dipole transitions is given by

$$S_{md}(aJ;bJ') = \mu_B^2 (f^N \alpha SLJ||\vec{L}+2\vec{S}||f^N \alpha' S'L'J')^2 \, , \tag{4}$$

where $\mu_B = e\hbar/2mc$.

The total radiative lifetimes were calculated from Eqs. (2)–(4) using eigenstates in an intermediate coupling scheme. These eigenstates are composed of linear combinations of SLJ states and usually exhibit only minor variations with host. Therefore matrix elements of $\underline{U}^{(\lambda)}$ and $\vec{L}+2\vec{S}$ in Eqs. (3) and (4) were taken from the literature and not calculated explicitly for $YAlO_3$. Electric dipole intensity parameters for rare earths in $YAlO_3$ were obtained from I.

The rms deviation between measured line strengths and line strengths calculated using the Judd-Ofelt approach is typically about 10–15%.[19] For J manifolds separated by small energy gaps, W is usually much greater than $\sum A_{ij}$ and hence is relatively unaffected by uncertainties in A. At the other extreme of large energy gaps, where $\sum A_{ij} \gg W$, uncertainties in A greatly affect the value and accuracy of W. This occurs, for example, for the first excited J states of lanthanide ions beyond Tb^{3+}. As an alternate approach, the spontaneous emission probability can be obtained from the integrated absorption cross section σ via the relationship

$$A(aJ;bJ') = \frac{8\pi n^2\nu^2}{c^2} \frac{2J'+1}{2J+1} \int \sigma(\nu)\, d\nu \quad . \tag{5}$$

Contributions to W also arise from nonradiative decay by ion-ion interactions. Self-quenching, for example, is observed from the concentration dependence of the Nd^{3+} $^4F_{3/2}$ and Ho^{3+} $^5S_2$ lifetimes in $YAlO_3$.[20] Generally, however, these processes are important only when pairs of near-resonant transitions are present and at fractional rare-earth concentrations $\gtrsim 1\%$. To avoid relaxation by ion-ion coupling, all measurements were made using samples containing the lowest rare-earth concentration available and consistent with signal-to-noise considerations.

The lifetimes of excited states which fluoresce were determined directly from the fluorescence decay following pulsed excitation. The lifetimes of excited states from which fluorescence was not readily detectable were determined by selectively exciting ions into these levels and then monitoring the transient fluorescence from a lower level.[21,22] For the simple case where a level 2 decays directly to a fluorescing level 1, the fluorescence will exhibit a maximum intensity at time

$$t_{max} = \frac{\ln(\tau_2/\tau_1)}{1/\tau_1 - 1/\tau_2} \quad , \tag{6}$$

where the excitation pulse is assumed to be very much shorter than τ_1 and τ_2. Hence, by measuring t_{max} and τ_1, the lifetime τ_2 is determined.

III. EXPERIMENTAL DETAILS

Crystals of $YAlO_3$ doped with rare earths were grown from stoichiometric melts using the Czochralski method[20] and subsequently heated in a reducing atmosphere to remove color centers. The purity of the starting materials was 99.99%. Quoted rare-earth concentrations are the nominal atomic percent substituted for yttrium. The samples were small single crystals with dimensions typically a few mm on a side. They were mounted in a quartz Dewar through which flowed dry nitrogen gas. By a combination of a liquid-nitrogen heat exchanger and a nichrome-wire heater, the gas temperature could be varied continuously from approximately 77 to 700 °K. The sample temperature was measured with a thermocouple in contact with the crystal.

Excited-state lifetimes were measured using apparatus and procedures similar to those described previously.[22] Ions were pumped into selected excited states by radiation from a xenon flashlamp-grating monochromator combination. The flashlamp had a pulse width [full width at half-maximum (FWHM)] of ≈1 μsec. In cases of very fast decays, a pulsed nitrogen lamp having a pulse duration of 10 nsec was used. Transient fluorescence signals were observed with a grating monochromator equipped with a *S*-20 or liquid-nitrogen-cooled *S*-1 photomultipler tube. For observing longer wavelengths beyond the range of the *S*-1 photomultiplier, another monochromator–PbS-detector combination was employed; the response time of the latter system was ~50 μsec.

Fluorescence decay signals were displayed on an oscilloscope and photographed. When necessary, the signal-to-noise ratio was improved by digital signal averaging (CAT-1024) or a PAR Wavefunction Eductor. The minimum sampling time available was 1 μsec, which set a limit on the decay rates measurable. Decays were, whenever possible, plotted over about three lifetimes and, unless noted otherwise, were fitted to a simple exponential decay law.

IV. EXPERIMENTAL RESULTS

Energy-level diagrams showing the pertinent levels for the five rare earths studied are given in Fig. 1 (the extent of the crystal-field splitting of the J manifolds is suppressed). At low temperatures, fluorescence was observed from levels marked by a solid semicircle. Since radiative transitions are not strictly forbidden, observation of fluorescence from other levels is a question of competition of radiative and nonradiative decay probabilities and detection sensitivity.

Detailed results for each ion investigated are presented below. The excited-state lifetimes and multiphonon emission rates given are those at liquid-nitrogen temperatures.

A. Neodymium

Fluorescence was observed from several levels of Nd^{3+}; however, the principal fluorescence occurs from the $^4F_{3/2}$ level.[23–25] The lifetime of this fluorescence is 175 μsec. The energy gap from $^4F_{3/2}$ to the next-lower level $^4I_{15/2}$ is ≈4700 cm^{-1}. As shown later, the estimated multiphonon emission rate is < 10 sec^{-1} and hence beyond the experimental accuracy of the present measurements. Calcula-

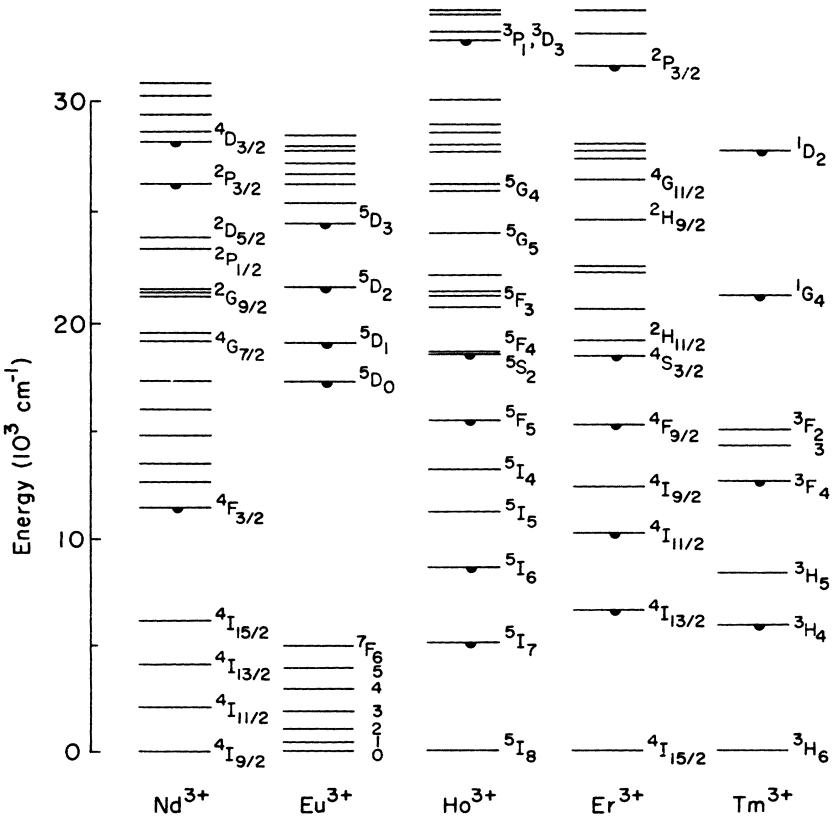

FIG. 1. Energy-level diagrams for the rare-earth ions studied. In $YAlO_3$, fluorescence was observed from levels marked by solid semicircles.

tions confirm that the radiative quantum efficiency of $^4F_{3/2}$ is near unity.[26]

The lifetimes of higher excited states were determined by monitoring the risetime of the $^4F_{3/2}$ fluorescence following pulsed selective excitation. A crystal containing 0.1-at.% Nd was examined. Using a xenon flashlamp, a lower limit of 10^6 sec^{-1} was found for the total decay rate at 77 °K to $^4F_{3/2}$ from states up to and including $^2D_{5/2}$ at ~24 000 cm^{-1}. The radiative decay probabilities from these states, though not calculated explicitly, are estimated to be $\lesssim 10^5$ sec^{-1}. The observed decay rate to $^4F_{3/2}$ is therefore attributed mainly to a level-by-level nonradiative cascade involving multiphonon emission. The largest energy gap to be bridged in this cascade is the 1390 cm^{-1} from the group of unresolved ($^4G_{7/2}$, $^4G_{9/2}$, $^2K_{13/2}$) states at ~19 000 cm^{-1}. Other large transitions of 1230 cm^{-1} occur from $^2G_{9/2}$ and $^2P_{1/2}$. In a further experiment, ions were excited into the ($^4G_{7/2}$, $^4G_{9/2}$, $^2K_{13/2}$) group of levels by a 10-nsec pulse at 0.53 μm from a frequency-doubled YAG:Nd laser. The resulting $^4F_{3/2}$ fluorescence at 300 °K reached a maximum intensity at 0.6±0.2 μsec after the laser pulse. From Eq. (6), the decay rate to $^4F_{3/2}$, extrapolated to 77 °K, is ~10^7 sec^{-1}. Since the step from $^4G_{7/2}$ is the largest in the cascade, this rate is ascribed to multiphonon emission for an energy gap of ≈1400 cm^{-1}.

When ions were excited into levels above $^2D_{5/2}$ using wavelengths ≤360 nm, the $^4F_{3/2}$ fluorescence peak occurred later. Using a simple equivalent three-level model and Eq. (6), a total effective decay rate of ~2×10^5 sec^{-1} was obtained. Since the decay rate from $^2D_{5/2}$ to $^4F_{3/2}$ is >10^6 sec^{-1}, this slower rate must arise principally from the decay to $^2D_{5/2}$. The largest energy gaps for multiphonon emission are $^2P_{3/2} \rightarrow {}^2D_{5/2}$ (2220 cm^{-1}) and $^4D_{3/2} \rightarrow {}^2P_{3/2}$ (1550 cm^{-1}). Both of these transitions are subject to limitations imposed by the triangle rule discussed later. Neglecting J mixing, only second-order terms in the ion-lattice interaction contribute to the $^4D_{3/2} \rightarrow {}^2P_{3/2}$ decay. However, based upon results for other ions, the above rate of 2×10^5 sec^{-1} appears to be much too slow for an energy gap of 1550 cm^{-1}. Therefore the rate is attributed predominantly to decay from $^2P_{3/2}$. The estimated radiative decay rate from $^2P_{3/2}$ is ~3.5×10^3 sec^{-1} and hence negligible.

B. Europium

Fluorescence was observed from $^5D_0$, $^5D_1$, $^5D_2$, and $^5D_3$ to levels of the ^7F ground multiplet. Ions excited into levels above $^5D_3$ decay rapidly ($\lesssim$1 μsec) to $^5D_3$ followed by a simple exponential decay from $^5D_3$. In addition to radiative decay, a stepwise $^5D_3 \rightarrow {}^5D_2 \rightarrow {}^5D_1 \rightarrow {}^5D_0$ cascade, similar to that reported for LaF_3:Eu^{3+},[8] was evident by observing the rise time and decay of successively lower levels. Selective excitation was employed to unravel the lifetimes. For example, to measure the $^5D_2$ lifetime, ions were selectively excited into $^5D_2$ and the decay of the $^5D_2 \rightarrow {}^7F_3$ fluorescence observed. Lifetimes measured at 77 °K for a sample containing 0.25-at.% Eu are listed in Table I. At this concentration, pairs of energy-conserving transitions of the types $^5D_J \rightarrow {}^5D_{J'}$: $^7D_{0,1} \rightarrow {}^7F_{J'}$ or $^5D_J \rightarrow {}^7F_{J'}$: $^7F_{0,1} \rightarrow {}^5D_{J'}$ are expected to make only a very small contribution to the total decay rates.

TABLE I. Observed lifetime, calculated radiative lifetime, and multiphonon decay rate for excited states of Eu^{3+} in $YAlO_3$ at 77 °K.

Excited state	Observed lifetime (μsec)	Radiative lifetime (μsec)	Multiphonon rate (sec^{-1})	Energy gap (cm^{-1})
$^5D_0$	1500	1400	~0	12 400
$^5D_1$	65	1610	1.5×10^4	1 750
$^5D_2$	≈25	1980	4×10^4	2 400
$^5D_3$	58	···	~1.6×10^4	2 700

Whereas the $^5D_0$ lifetime was independent of temperature from 77 to 700 °K, the $^5D_1$, $^5D_2$, and $^5D_3$ lifetimes varied with temperature. In $LaAlO_3$, nonradiative decay of excited Eu^{3+} ions via charge transfer states at 32 000 cm^{-1} has been reported.[27] No evidence of low-lying charge transfer bands and associated relaxation effects were observed for Eu^{3+} in $YAlO_3$.

The spontaneous emission probability for $^5D_0 \rightarrow {}^7F_1$ magnetic dipole transitions, calculated using eigenstates in intermediate coupling[9] and neglecting J mixing, is 107 sec^{-1}. Combining this result with the measured fluorescence branching ratios, yields a total radiative lifetime for $^5D_0$ of 1.4 msec. Within experimental uncertainties, this value is in good agreement with the observed lifetime of 1.5 msec, thereby indicating a quantum efficiency of unity. Calculated radiative lifetimes for $^5D_1$ and $^5D_2$ are included in Table I. Although J mixing was neglected, the results are sufficient to demonstrate that radiative transitions constitute only a small fraction (< 10%) of the total decay rates. Calculations for $^5D_3$ were not made because J mixing is important and the required matrix elements were not available. It seems reasonable to assume, based upon the radiative decay rates for $^5D_1$ and $^5D_2$, that the radiative lifetime of $^5D_3$ will be in the order of 1 msec. Since this is very small compared to the observed lifetime, any error in the multiphonon decay rate made using this estimate should also be small.

TABLE II. Observed lifetime, calculated radiative lifetime, and multiphonon decay rate for excited states of Ho^{3+} in $YAlO_3$ at 77 °K.

Excited state	Observed lifetime (μ sec)	Radiative lifetime (μsec)	Multiphonon rate (sec^{-1})	Energy gap (cm^{-1})
$^5I_7$	6600	6400	$\lesssim 10$	4700
$^5I_6$	465	2990	1.8×10^3	3200
$^5F_5$	$\lesssim 3$	235	$\gtrsim 3.3\times10^5$	2100
$^5S_2$	62	169	1.1×10^4	2800
$^5F_3$	~1	133	$\sim 1\times10^6$	1850
$^3P_1, ^3D_3$	9	158	1.0×10^5	~2400

C. Holmium

The lifetimes of five excited states were measured directly from their fluorescence decay. The lifetime of the $^5F_3$ state was derived from the risetime of the $^5S_2$ fluorescence following excitation with a pulsed nitrogen lamp. The lifetime results for a 0.2-at.% Ho sample are summarized in Table II. Because of the small absorption cross sections for transitions from $^5I_8$ to $^5I_5$ and $^5I_4$, direct excitation and observation of the $^5I_5$ and $^5I_4$ lifetimes are difficult and no useful data were obtained.

Calculations of the radiative decay probabilities from excited states of Ho^{3+} are described in a separate paper[28]: the predicted radiative lifetimes are included in Table II. Since the agreement between the calculated and observed intensities for the $^5I_8 \rightarrow {}^5I_7$ transition, which has a significant magnetic dipole contribution, was comparatively poor, the radiative lifetime for $^5I_7$ was determined instead from Eq. (5). Some uncertainty in this result arises because at 300 °K the Stark levels of the initial $^5I_8$ manifold in absorption and the $^5I_7$ manifold in emission are not equally populated. For the $^5S_2$, $^3F_3$, and ($^3P_1$, $^3D_3$) states, J mixing with nearby states may affect the accuracy of the calculated radiative lifetimes. The radiative lifetimes, however, are all much longer than the total lifetimes, hence any errors arising from the neglect of J mixing should not have a significant effect on the derived multiphonon emission rates.

D. Erbium

Transient fluorescence from five excited states of Er^{3+} ($^4I_{13/2}$, $^4I_{11/2}$, $^4F_{9/2}$, $^4S_{3/2}$, $^2P_{3/2}$) was studied. A search was made at 77 °K for transient emission from $^4G_{11/2}$, which is predicted to have a large radiative decay probability, but none was detected. Lifetime measurements were made using crystals containing 0.5- or 1-at.% Er; in instances where concentration quenching by ion-pair interactions might be significant, such as for $^4S_{3/2}$, a sample containing ~0.1-at.% Er was used. The lifetime of $^2H_{9/2}$ was determined by pumping into the ($^4G_{11/2}$, $^2G_{7/2}$, $^2G_{9/2}$, $^2K_{15/2}$) group of levels at ≈360–380 nm and measuring the risetime of the $^4S_{3/2}$ fluorescence. Since the $^2H_{9/2} \rightarrow {}^4F_{3/2}$ transition has the largest energy gap in a level-by-level cascade to $^4S_{3/2}$, it was assumed to be the rate-limiting step. The limiting lifetime of $^4D_{5/2}$ at ≈38,000 cm^{-1} was estimated from the rise time of the $^2P_{3/2}$ fluorescence. The measured Er^{3+} lifetimes are presented in Table III.

The lifetimes at 300 °K of the lower levels of Er^{3+} were reported earlier.[29] The present lifetimes at 77 °K are in reasonable agreement with these results. The $^4I_{13/2}$ lifetime at 300 °K is longer than that at 77 °K, but may have been lengthened by radiation trapping because previously a larger sample was used.

Calculated radiative lifetimes[30] are included in Table III. Of the seven excited states considered, only five yield results useful for determining the dependence of the multiphonon emission rate on energy gap. Because of the large $^4I_{13/2}$-$^4I_{15/2}$ energy difference, decay of $^4I_{13/2}$ by multiphonon emission should be negligibly small compared to the radiative rate; the radiative and total lifetimes do indeed agree within experimental error. In the case of $^2P_{3/2}$, although some multiphonon emission may be present, its rate is probably smaller than the ~15–20% uncertainty in the calculated radiative lifetime. Finally, it should be noted that the radiative lifetime of $^4S_{3/2}$ was calculated neglecting J mixing with $^2H_{11/2}$; however, the radiative rate from $^2H_{11/2}$ is larger than from $^4S_{3/2}$.

E. Thulium

Fluorescence was readily observed from five J manifolds: $^3H_4$, $^3F_4$, $^1G_4$, $^1D_2$, and $^3P_0$. With the

TABLE III. Observed lifetime, calculated radiative lifetime, and multiphonon decay rate for excited states of Er^{3+} in $YAlO_3$ at 77 °K.

Excited state	Observed lifetime (μsec)	Radiative lifetime (μsec)	Multiphonon rate (sec^{-1})	Energy gap (cm^{-1})
$^4I_{13/2}$	5300	4400	···	6125
$^4I_{11/2}$	1220	4400	5.9×10^2	3425
$^4F_{9/2}$	19	280	4.9×10^4	2530
$^4S_{3/2}$	160	380	3.6×10^3	2950
$^2H_{9/2}$	1.2	190	8.3×10^5	1950
$^2P_{3/2}$	49	37	···	3375
$^4D_{5/2}$	$\lesssim 1$	71	$\gtrsim 10^6$	1750

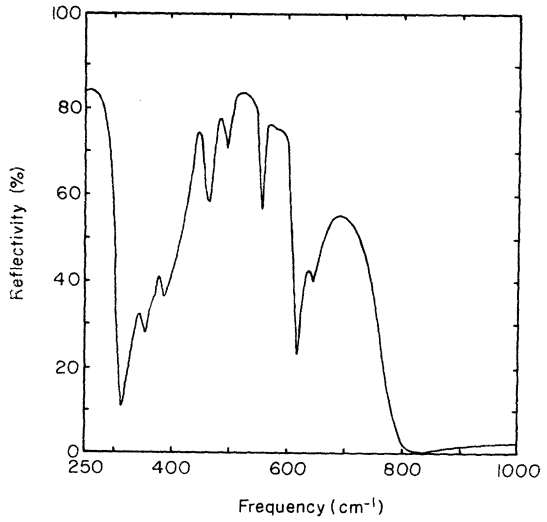

FIG. 2. Infrared reflection spectrum of $YAlO_3$ at 300 °K.

exception of $^3F_4$, the energy gaps from those levels to the next-lower levels are all $\gtrsim 5000$ cm^{-1} and hence the decays are predominantly radiative. The $^3F_3$ and $^3H_5$ states, which have energy gaps to $^3F_4$ and $^3H_4$, respectively, of 1500 and 2275 cm^{-1}, should decay predominantly by multiphonon emission. Although the associated rates are in principle observable from the rise time of the $^3H_4$ and $^3F_4$ fluorescences following pulsed selective excitation into $^3F_3$ and $^3H_5$, in both cases the expected rates were beyond the time resolution available in our experiments. Therefore only a single multiphonon emission rate datum was obtained for Tm^{3+}, that of $^3F_4$.

The radiative probability from $^3F_4$ to the $^3H_6$ ground state was determined from Eq. (5) and the integrated absorption cross section measured using a 1-at.% Tm crystal at room temperature. The resulting value of A from Eq. (5) was 1030 sec^{-1}. The fluorescence branching ratio for $^3F_4 \rightarrow {}^3H_6$, calculated using matrix elements derived for $Tm^{3+}:Y_2O_3$[9] and the Judd-Ofelt parameters given in I, is 0.84. The total estimated radiative decay probability, including all magnetic and electric dipole transitions, is 1230 sec^{-1}.

The lifetime of the $^3F_4$ fluorescence was measured for a crystal containing 1-at.% Tm, the only sample available. For thulium-doped Y_2O_3[9] and YF_3,[31] the $^3F_4$ lifetime is concentration dependent. In these hosts, the $^3F_4$ lifetime at thulium concentrations of 1 at.% is reduced to about one-half of its value at low concentrations ($\lesssim 0.1$ at.%) due to quenching by Tm^{3+}-Tm^{3+} interactions. Since the ion densities for Tm-doped $YAlO_3$ are not too different from those in the other two hosts, a similar concentration dependence is expected. The concentration independent lifetime for $^3F_4$ in $YAlO_3$ is estimated to be ~700 μsec.[32] Combining this with the radiative rate above yields a multiphonon decay rate of ~200 sec^{-1} for the $^3F_4$-$^3H_5$ energy gap of 3800 cm^{-1}. This rate is small compared to the total decay rate and hence is sensitive to the latter value. For example, if $\tau(^3F_4) \sim 600$ μsec, $W \sim 400$ sec^{-1}; if $\tau(^3F_4) \sim 800$ μsec, $W \sim 10$ sec^{-1}. Because of the uncertainty in the exact value of the lifetime, only the order of magnitude of the $^3F_4$ multiphonon rate datum is significant.

V. DISCUSSION

A. Phonon Spectrum and Ion-Lattice Coupling

The magnitude and temperature variation of multiphonon emission rates are dependent upon the phonon frequency distribution and the strength of the ion-lattice coupling. Information about these properties can be obtained from infrared, Raman, and vibronic spectra. The infrared reflectivity spectrum of $NdAlO_3$ has been reported.[33] (Whereas the lighter rare-earth orthoaluminates including Nd have trigonal D_{3d}^6 symmetry, $YAlO_3$ and heavier rare-earth orthoaluminates beginning with $SmAlO_3$ have orthorhombic D_{2h}^{16} symmetry.) From an analysis of the $NdAlO_3$ spectrum, transverse and longitudinal optic-mode frequencies ranging up to 676 and 766 cm^{-1}, respectively, were found. The infrared reflectivity spectrum of $YAlO_3$, recorded at 300 °K using a Perkin Elmer 457 spectrophotometer, is shown in Fig. 2. The general features of this spectrum are similar to and the frequencies of the reflectivity peaks are only slightly different from those for $NdAlO_3$. Therefore the highest optical-phonon frequencies for $YAlO_3$ should be comparable to those above for $NdAlO_3$.

The Raman spectrum of $YAlO_3$ is complex. Polarized spectra recorded[34] for several crystal orientations at 300 °K reveal many intense lines between ≈ 145 and 550 cm^{-1}. A weak line was observed at 685 cm^{-1} and a very weak peak at 740 cm^{-1}. In $SmAlO_3$, a broad line is reported at 601 cm^{-1}.[35]

Vibronic spectra provide further evidence of the extent of the phonon spectrum. In addition, the intensity is proportional to a product of the mode density and the coupling strength of the various phonons.[36] Of rare earths in $YAlO_3$, vibronic sidebands are most prominent in the spectra of Yb^{3+}.[37] In Fig. 3, the excitation spectrum of the Yb^{3+} $^2F_{5/2} \rightarrow {}^2F_{7/2}$ fluorescence is shown for a powdered sample at 77 °K. Purely electronic transitions from the ground state are denoted by (e). The line at 979 nm corresponds to the transition between the lowest Stark levels of $^2F_{7/2}$ and $^2F_{5/2}$; other peaks are attributed to phonon-assisted transitions and are measured with respect to the 979-nm line. A clearer vibronic spectrum accompanies the R-line fluorescence of Cr^{3+} in $YAlO_3$

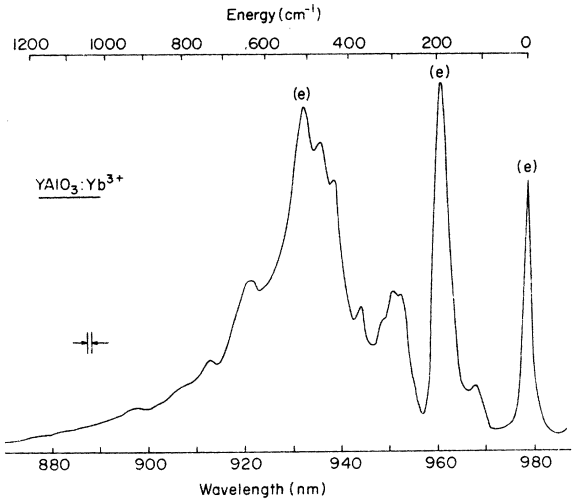

FIG. 3. Excitation spectrum of the $^2F_{5/2} \rightarrow {}^2F_{7/2}$ fluorescence of Yb^{3+} in $YAlO_3$ at 77 °K. The three purely electronic transitions from the ground state are denoted by (*e*).

and is shown in Fig. 4. Since chromium ions reside at Al^{3+} sites whereas rare earths occupy Y^{3+} sites, the coupling of vibrations to ions at the two sites will not be identical. Nevertheless, the overall vibronic intensity distributions in Figs. 3 and 4 are similar. The strongest lines occur between about 300 and 500 cm^{-1}. High-energy peaks at 600–650 cm^{-1} and ~740 cm^{-1} are observed in both spectra. Weak vibronics at higher energies in Fig. 3 are most probably due to multiple-phonon bands (this could also be the origin of the weak lines at 740 cm^{-1}).

Detailed analyses of the above spectra are beyond the scope of this paper. The results indicate, however, that (i) phonon energies in $YAlO_3$ range up to approximately 650–750 cm^{-1}; (ii) the most numerous and/or most strongly coupled phonons have energies of ~450–500 cm^{-1}.

B. Energy-Gap Dependence

The ion-lattice interaction for 4*f* electrons is characteristic of weak coupling. Studies of multiphonon relaxation of rare earths in several materials have shown[2] that the rate at low temperatures exhibits an approximately exponential dependence on the energy gap ΔE to the next-lower level of the form

$$W = W(0)e^{-\alpha \Delta E} . \qquad (7)$$

The constants $W(0)$ and α in Eq. (7) are found to be dependent of the host crystal and strength of ion-lattice coupling but, with rare exceptions, independent of the specific rare-earth ion or electronic states involved.

Data on the multiphonon emission rates in $YAlO_3$ at 77 °K are plotted semilogarithmically versus energy gap to the next-lower level in Fig. 5. To account for the thermal Boltzmann populations of higher-lying levels of the initial *J* manifold at 77 °K, the energy gaps to the next-lower level were taken to be slightly larger ($\sim kT/2$) than the minimum gap between Stark levels of the two *J* manifolds.[38] As seen from Fig. 5, the rates for five different ions and fifteen different excited states can be fitted approximately (within a factor of ~2) by a simple exponential dependence on the energy gap given by Eq. (7) with $W(0) = 5\times10^9$ sec^{-1} and $\alpha = 4.6 \times 10^{-3}$ cm. (The two exceptions, the $^5D_1$ and $^5D_2$ states of Eu^{3+}, are subject to selection-rule restrictions discussed below.) As noted earlier, the data for very small and very large energy gaps have large uncertainties; although not quantitatively useful, they are, nevertheless, consistent with the over-all trend. For the range of energy gaps studied, a minimum of three phonons and upwards to seven phonons are active in the relaxation. These results for $YAlO_3$ therefore attest again to the averaging out of the detailed features of the electronic states and phonon modes in these high-order processes.

The exponential dependence in Eq. (7) is an approximation of the dependence predicted by more detailed treatments.[4] While applicable to processes involving many phonons, it must eventually break down for small energy gaps where relaxation by one- or two-phonon processes is possible. In this regime, the statistical averaging that occurs for high-order processes is no longer prominent; relaxation rates are strongly dependent on the phonon density of states and coupling at given frequencies. This behavior is displayed by the relative linewidths observed at low temperatures for transitions terminating on Stark levels of a single *J* manifold. Be-

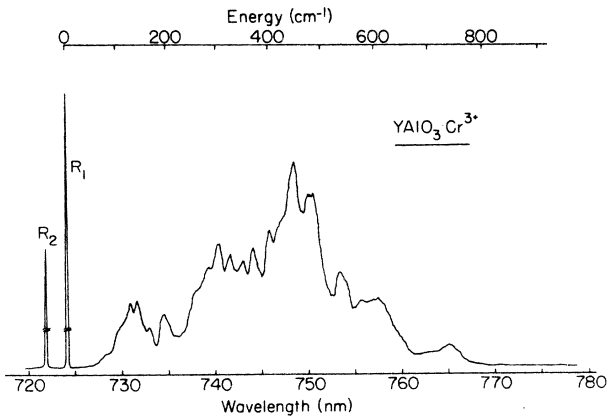

FIG. 4. Vibronic spectrum associated with the $^2E \rightarrow {}^4A_2$ fluorescence of Cr^{3+} in $YAlO_3$ at 77 °K. The *R* lines were recorded using reduced gain.

cause of rapid relaxation by one-phonon direct or two-phonon Raman or Orbach processes, the highest-lying levels on a manifold are usually lifetime broadened.[39] For example, in $YAlO_3:Nd^{3+}$ the linewidths for fluorescence to $^4I_{9/2}$ at 85 °K range from ~1 cm^{-1} for the lowest level to 35 and 19 cm^{-1} for the two highest levels at 491 and 669 cm^{-1}.[26] The former width is governed by inhomogeneous broadening, the latter two by lifetime broadening. Extrapolation of the results in Fig. 5 to energy gaps ≤ 699 cm^{-1} yields relaxation rates of $\lesssim 5\times10^9$ sec^{-1}. Considering transitions to all possible terminal levels within the manifold, the associated lifetime broadening is less than 1 cm^{-1}; hence Eq. (7) is no longer adequate.

The results in Fig. 5 are useful in predicting energy-decay schemes and when fluorescence may be anticipated and in estimating quantum efficiencies and lattice heating associated with multiphonon emission. An important question for four-level operation of $YAlO_3:Nd^{3+}$ lasers[20] is the lifetime of the $^4I_{11/2}$ terminal state. Since the minimum energy gap from $^4I_{11/2}$ to $^4I_{9/2}$ at 300 °K is 1350 cm^{-1}, an extrapolation of Fig. 5 yields a $^4I_{11/2}$ lifetime of ~10^{-7} sec. Because energy can be conserved by the creation of only two or three phonons, the comments made above may be apropos.

C. Selection Rules

The ion-lattice interaction is composed of a product of operators for electronic transitions and for phonon creation and annihilation. Since the transitions of interest are between electronic states of a given f^n configuration, they involve no change in parity between the initial and final states. Hence only those terms in the expansion of the ion-lattice interaction which are of even order will be important. For an electronic operator of rank r, there is a triangle rule governing possible initial and final J states given by

$$|J-J'| \leq r \leq |J+J'| \quad , \tag{8}$$

where for lanthanide-series ions, $r \leq 6$. J mixing acts to relax this triangle rule.

The ion-lattice interaction is also subject to a spin selection rule $\Delta S = 0$. Because of admixing of spin states by the spin-orbit interactions, S is generally not a good quantum number which reduces

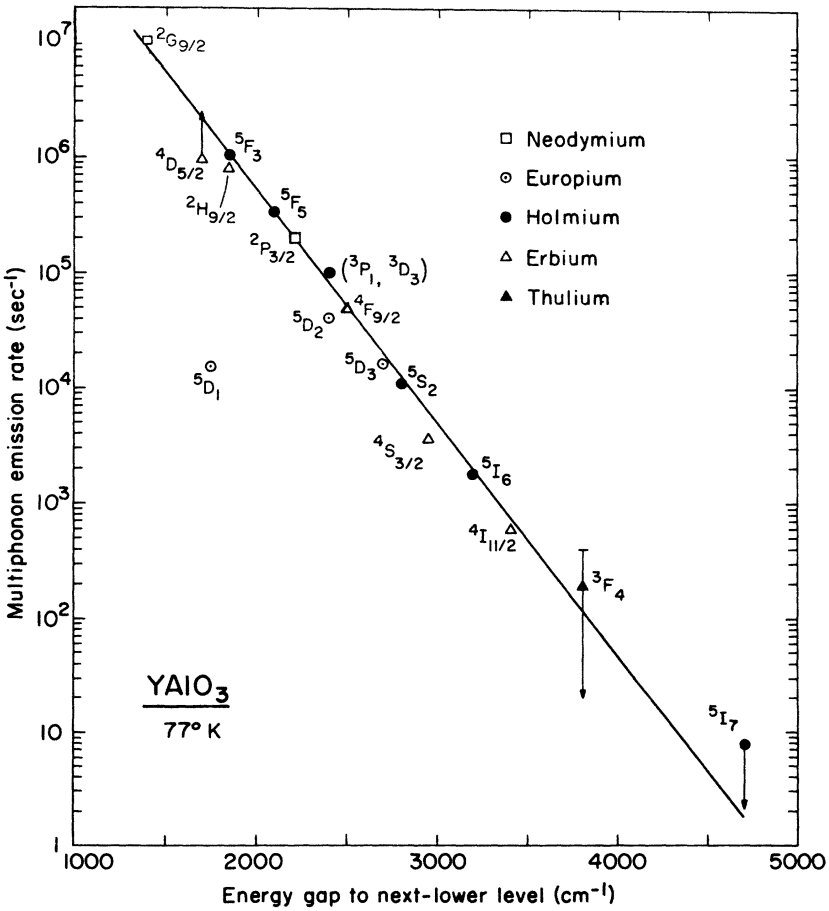

FIG. 5. Dependence of the rate of multiphonon emission on energy gap to the next-lower level for excited states of rare-earth ions in $YAlO_3$ at 77 °K.

the importance of this rule.

The selection rule in Eq. (8) is a serious restriction for multiphonon relaxation of rare earths in only a very few cases, such as $^5D_0 \rightleftharpoons {}^5D_1$ and $^7F_0 \rightleftharpoons {}^7F_1$ (Eu^{3+} and Tb^{3+}) and $^3P_0 \rightleftharpoons {}^3P_1$ (Pr^{3+} and Tm^{3+}). These transitions are formally forbidden and occur either due to J mixing or higher-order processes. Of these, the $^5D_1 \rightarrow {}^5D_0$ transition of Eu^{3+} is readily amenable to study and reduced rates of multiphonon emission have been observed.[8,9] In $YAlO_3$, the $^5D_1$ rate of Eu^{3+} is two orders of magnitude less than that predicted for states having comparable energy gaps in Fig. 5.

There are several instances where under the above conditions only one even-order term in the ion-lattice interaction is active for multiphonon relaxation. These include $^4F_{3/2} \rightarrow {}^4I_{15/2}$ and $^4D_{3/2} \rightarrow {}^2P_{3/2}$ (Nd^{3+}), $^3P_0 \rightarrow {}^1D_2$ (Pr^{3+}), $^6F_{1/2} \rightarrow {}^6H_{13/2}$ (Sm^{3+}), $^5D_2 \rightarrow {}^5D_1$ (Eu^{3+}), $^7F_1 \rightleftharpoons {}^7F_2$ (Eu^{3+}, Tb^{3+}), $^3M_{10} + {}^3L_8 \rightarrow {}^3D_3 + {}^3P_1$ (Ho^{3+}), and $^2K_{13/2} \rightarrow {}^2P_{3/2}$ (Er^{3+}). Unless the allowed terms are unusually large, a slower multiphonon decay rate is expected for these transitions. As evident for the $^5D_2$ state, the reduction is not much more than a factor of 2 to 3. There are numerous cases where only second- and fourth- or fourth- and sixth-order terms are allowed, such as $^2P_{3/2} \rightarrow {}^2D_{5/2}$ (Nd^{3+}), $^5D_3 \rightarrow {}^5D_2$ (Eu^{3+}), $^3P_1 + {}^3D_3 \rightarrow {}^3D_2$ (Ho^{3+}), and $^4S_{3/2} \rightarrow {}^4F_{9/2}$ (Er^{3+}). With the exception of $^4S_{3/2}$, the measured multiphonon emission rates from these states in $YAlO_3$ are not significantly beyond the normally observed variations from the exponential dependence. As noted above J mixing may be important in some instances.

D. Temperature Dependence

The lifetimes of many excited states are temperature dependent. This can arise from several sources: a changing population distribution among Stark levels having different radiative and nonradiative decay probabilities, stimulated multiphonon emission, or vibronic transitions. (Relaxation by energy migration and transfer may also be temperature dependent but these processes are assumed to be unimportant for low rare-earth concentrations.) Since the Stark levels within a J manifold rapidly come into thermal equilibrium, the temperature dependence of the effective J manifold lifetime is given by

$$\frac{1}{\tau} = \frac{\sum_i \sum_j g_i [A_{ij}(T) + W_{ij}(T)] e^{-E_i/kT}}{\sum_i g_i e^{-E_i/kT}} , \qquad (9)$$

where g_i and E_i are the degeneracy and energy of the ith level within the manifold and the summation is over all terminal levels j. Although radiative transition probabilities between individual pairs of Stark levels are not equal, when many initial and final levels are involved, variations in the total radiative decay rate due to changing level populations tend to be small. It is confirmed by the observed temperature-independent lifetimes of J states where the energy gap to the next-lower state is sufficiently large to rule out multiphonon emission (examples include the $^4F_{3/2}$ state of Nd^{3+},[20] the $^5D_4$ and $^5D_3$ states of Tb^{3+},[28] and the $^1D_2$ state of Pr^{3+}). Thermally populating higher J states which have significantly different radiative decay rates, such as for the $^4S_{3/2}$ and $^2H_{11/2}$ states of Er^{3+} and $^3P_0$ and $^3P_1$ states of Pr^{3+}, can be important, however.

Vibronic transitions are generally most intense for ions near the beginning or end of the $4f^n$ series. Even for Yb^{3+}, however, the $^2F_{5/2}$ lifetime varies less than 10% over the temperature range 77–700 °K.[37] Therefore, temperature-dependent vibronic transitions are considered to make a negligibly small contribution to the lifetimes studied.

Under the above assumptions, the temperature dependence of the multiphonon emission rates was found by simply subtracting the calculated radiative rate from the measured lifetime at each temperature. Lifetimes investigated were $^4I_{11/2}$ (Er^{3+}), $^5I_6$ (Ho^{3+}), and $^5D_3$ (Eu^{3+}). These states were selected because (i) W was $\gtrsim A$, (ii) τ could be measured over a large temperature range, and (iii) the J manifold was, except for $^5D_3$, well isolated. The resulting temperature dependences are plotted in Figs. 6 and 7.

The highest-energy phonons are usually considered to make the dominant contribution to multiphonon relaxation since they conserve energy in the lowest-order process.[2] For relaxation by emission of phonons of a single frequency ν, where

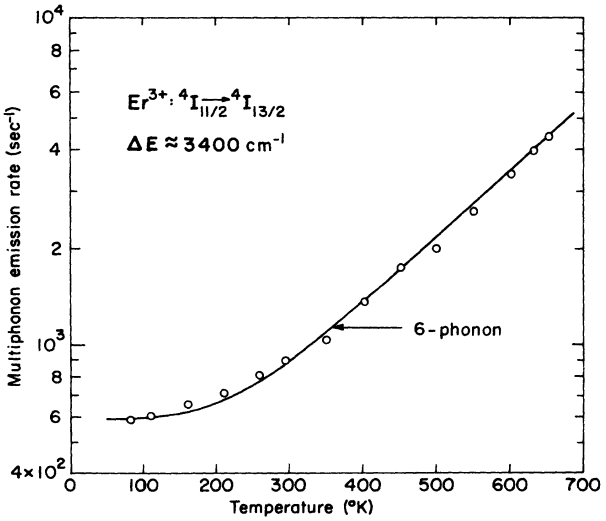

FIG. 6. Measured temperature dependence of the Er^{3+} $^4I_{11/2} \rightarrow {}^4I_{13/2}$ multiphonon emission rate. The curve was calculated from Eq. (10) assuming relaxation by six 570-cm^{-1} phonons.

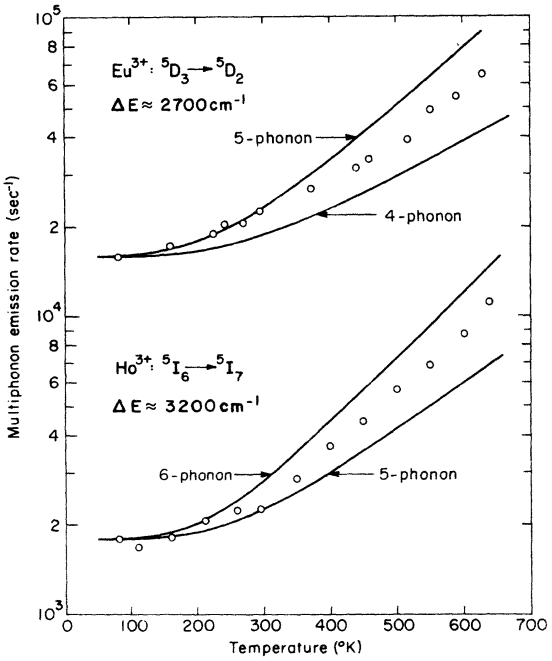

FIG. 7. Observed temperature dependences of the Eu^{3+} $^5D_3 \rightarrow {}^5D_2$ and Ho^{3+} $^5I_6 \rightarrow {}^5I_7$ multiphonon emission rates. The curves represent temperature dependences calculated from Eq. (10) assuming relaxation by different multiples of single-phonon frequencies consistent with energy conservation.

$\nu \approx \nu_{max}$, the order of the process required to bridge an energy gap ΔE is $n = \Delta E/h\nu$. The temperature dependence for an n-phonon process using this single-frequency model is given by

$$W_n(T) = W_n(0)(1 - e^{-h\nu/kT})^{-n} , \qquad (10)$$

where $W(0)$ is the spontaneous emission probability. If one used the highest-energy phonons in $YAlO_3$ (~700–750 cm^{-1}), this model does not fit the observed temperature dependences. Better fits to the data are obtained using larger numbers of lower-energy phonons consistent with energy conservation. By considering six 570-cm^{-1} phonons, the multiphonon emission rate for $^4I_{11/2}$ is accounted for over the entire temperature range in Fig. 6.

When theoretical curves derived from Eq. (10) are applied to the data in Fig. 7, satisfactory agreement is not obtained over the full temperature range studied. For these cases the single-frequency model may be too great an oversimplification. As Kisluik and Moore[40] have pointed out, processes involving lower-frequency phonons, being of higher order, have steeper temperature dependences and hence should govern the relaxation at sufficiently high temperatures. A weighted average over the phonon spectrum would therefore be more appropriate. Others have achieved agreement with experiment by considering the thermal population of higher-lying levels of the initial J manifold.[2,5,6,41] While such refinements might lead to improved fits for the present data, they did not seem warranted in view of the totality of uncertainties arising from the assumptions made and the experimental accuracy.

The analysis of the temperature dependences, while admittedly not detailed, does indicate that multiphonon relaxation of rare earths in $YAlO_3$ is not dominated solely by the highest-energy phonons. (A similar conclusion was reached for multiphonon relaxation in $Y_3Al_5O_{12}$.[12]) Lower-energy phonons or combinations of phonons in the range 550–650 cm^{-1} appear to be important. Although these phonons necessitate a higher-order process, the associated rate is probably larger because, as evident from the vibronic spectra, they are more numerous and/or more strongly coupled to rare-earth impurities.

As a further test, consider the relaxation of the $^5I_7$ state of Ho^{3+}. The $^5I_7$-$^5I_8$ energy gap is 4700 cm^{-1}, and hence the predicted spontaneous multiphonon rate from Fig. 5 is $\approx 2\ sec^{-1}$. For an estimate, assume relaxation occurs by eight 590-cm^{-1} phonons. Then at 600 °K, from Eq. (10), $W \approx 9W(0)$ $\approx 18\ sec^{-1}$. This is only ~10% of the observed lifetime and hence consistent with experimental results. In the case of the $^4F_{3/2} \rightarrow {}^4I_{15/2}$ transition of Nd^{3+}, where the energy gap is again 4700 cm^{-1}, the multiphonon emission would be negligible compared to radiative decay, in agreement with the observed temperature-independent lifetime.[20]

ACKNOWLEDGMENTS

I wish to thank Thomas Varitimos for his competent assistance in performing the experiments and in the initial data reduction, Mrs. B. Matsinger for her help in calculating radiative decay probabilities, and E. Comperchio and A. Morrison for growing the crystals used in these studies.

*Research supported in part by the U. S. Air Force Materials Laboratory, Dayton, Ohio and the Army Night Vision Laboratory, Ft. Belvoir, Va.

[1]A. Kiel, in *Quantum Electronics*, edited by P. Grivet and N. Bloembergen (Columbia U. P., New York, 1964), Vol. 1, p. 765.
[2]L. A. Riseberg and H. W. Moos, Phys. Rev. **174**, 429 (1968).
[3]T. Miyakawa and D. L. Dexter, Phys. Rev. B **1**, 2961 (1970).
[4]F. K. Fong, S. L. Naberhuis, and M. M. Miller, J. Chem. Phys. **56**, 4020 (1972).
[5]W. D. Partlow and H. W. Moos, Phys. Rev. **157**, 252 (1967).
[6]L. A. Riseberg, W. A. Gandrud, and H. W. Moos, Phys. Rev. **159**, 262 (1967).
[7]M. J. Weber, Phys. Rev. **157**, 262 (1967).

[8]M. J. Weber, in *Optical Properties of Ions in Crystals*, edited by H. M. Crosswhite and H. W. Moos (Interscience, New York, 1967), p. 467.
[9]M. J. Weber, Phys. Rev. **171**, 283 (1968).
[10]M. J. Weber, J. Chem. Phys. **48**, 4774 (1968).
[11]H. W. Moos, J. Lumin. 1, 2, 106 (1970).
[12]G. M. Zverev, G. Ya. Kolodnyi, and A. M. Onishchenko, Zh. Eksp. Teor. Fiz. **60**, 920 (1971) [Sov. Phys.-JETP **33**, 497 (1971)].
[13]M. J. Weber, T. E. Varitimos, and B. H. Matsinger, preceding paper, Phys. Rev. B 8, 47 (1973).
[14]K. H. Hellwege, Naturwissenschaften **34**, 212 (1947).
[15]B. Rinck, Z. Naturforsch. **3**, 406 (1948).
[16]J. R. Chamberlain, D. H. Paxman, and J. L. Page, Proc. Phys. Soc. Lond. **89**, 143 (1966).
[17]B. R. Judd, Phys. Rev. **127**, 750 (1962).
[18]G. S. Ofelt, J. Chem. Phys. **37**, 511 (1962).
[19]W. F. Krupke, Phys. Rev. **145**, 325 (1966).
[20]M. J. Weber, M. Bass, K. Andringa, R. R. Monchamp, and E. Comperchio, Appl. Phys. Lett. **15**, 342 (1969).
[21]S. A. Pollack, J. Chem. Phys. **38**, 2521 (1963).
[22]M. J. Weber, Phys. Rev. **156**, 231 (1967).
[23]Weak fluorescence was observed in the visible from higher excited states. Since emission has been reported from the $^2P_{3/2}$ (Ref. 24) and $^4D_{3/2}$ (Ref. 25) levels of Nd^{3+} in $Y_3Al_5O_{12}$, the visible emission of Nd:$YAlO_3$ probably also originates from one or both of these levels.
[24]V. L. Donlan (private communication).
[25]Yu. K. Voron'ko, B. I. Denker, V. V. Osiko, A. M. Prokhorov, and M. I. Timoshechkin, Dokl. Akad. Nauk SSSR **188**, 1258 (1969) [Sov. Phys.-Dokl. **14**, 998 (1970)].
[26]M. J. Weber and T. E. Varitimos, J. Appl. Phys. **42**, 4996 (1971).
[27]G. Blasse, A. Bril, and J. A. dePoorter, J. Chem. Phys. **53**, 4450 (1970).
[28]M. J. Weber, B. Matsinger, V. L. Donlan, and G. T. Surratt, J. Chem. Phys. **57**, 562 (1972).
[29]M. J. Weber, M. Bass, and G. A. deMars, J. Appl. Phys. **42**, 301 (1971).
[30]Matrix elements were obtained from Ref. 7.
[31]F. W. Ostermayer, Jr., J. P. van der Ziel, H. M. Marcos, L. G. Van Uitert, and J. E. Geusic, Phys. Rev. B **3**, 2698 (1971).
[32]A lifetime of 630 μsec has been reported: L. M. Hobrock, L. G. DeShazer, W. F. Krupke, G. A. Keig, and D. E. Witter, in Digest of Technical Papers, VII International Quantum Electronics Conference, 1972 (unpublished).
[33]P. Alain and B. Pirion, Phys. Status Solidi B **43**, 669 (1971).
[34]Raman spectra were recorded by Dr. K. Kizer of the Jarrell-Ash Division, Fisher Scientific Co.
[35]J. F. Scott and J. P. Remeika, Phys. Rev. B **1**, 4182 (1970).
[36]N. B. Manson, Phys. Rev. B **4**, 2645 (1971), and references therein.
[37]M. J. Weber, Phys. Rev. B **4**, 3153 (1971).
[38]Energy levels were either measured directly or supplemented by data from the following sources: Nd^{3+}, Ref. 26; Ho^{3+}, L. A. Riseberg (private communication); Er^{3+}, V. L. Donlan and A. A. Santiago, Jr., J. Chem. Phys. **57**, 4717 (1972); Tm^{3+}, L. M. Hobrock and L. DeShazer (private communication).
[39]W. M. Yen, W. C. Scott, and A. L. Schawlow, Phys. Rev. **136**, A271 (1964).
[40]P. Kisliuk and C. A. Moore, Phys. Rev. **160**, 307 (1967).
[41]F. K. Fong and M. M. Miller, Chem. Phys. Lett. **10**, 408 (1971).

PHYSICAL REVIEW B VOLUME 8, NUMBER 1 1 JULY 1973

Doubly Bottlenecked EPR in Cu:Cr,Mn

L. L. Hirst
Institut Max von Laue-Paul Langevin, 8046 Garching, West Germany

W. Schäfer, D. Seipler, and B. Elschner
Physikalisches Institut der Technischen Hochschule, 6100 Darmstadt, West Germany

(Received 27 December 1972)

The temperature dependence of the EPR linewidth in Cu : Cr,Mn has been measured. A generalization of the Hasegawa theory for the case with two species of paramagnetic impurities is derived and found to exhibit two interconnected bottleneck conditions. Our data indicate that Cu : Cr,Mn is doubly bottlenecked, i.e., that both Cr and Mn participate dynamically in the EPR.

I. INTRODUCTION

The EPR of Cr as an impurity in a metal has never been observed by conventional reflection-spectroscopy techniques, but a resonance with $g = 2.006$ has been seen by the very sensitive transmission-resonance method.[1] This experiment implies a spin-lattice relaxation rate of 2×10^9 sec^{-1} for Cr, which is considerably larger than that observed for Mn impurities.[2-5] This fact and the low solubility of Cr in Cu are presumably the reasons why the reflection-spectroscopy EPR of Cu:Cr has not been detected.

In the work reported here, we have overcome this difficulty by studying the EPR of Cu:Cr, Mn, where the Mn makes the observation of EPR possible. We have developed a generalized form of the Hasegawa bottlenecking theory,[6] which implies that under appropriate circumstances a doubly bottlenecked behavior can result such that both species of impurities participate dynamically in the EPR. Our data show that this behavior occurs in the case of Cu:Cr, Mn as indicated by the fact that the addition of Cr causes relatively little broadening of the linewidth. This should be contrasted with previously studied[5] systems such as